

# Crystal field, spin-orbit coupling and magnetism in a ferromagnet $\text{YTiO}_3$ <sup>♠</sup>

R. J. Radwanski

Center of Solid State Physics, *S<sup>nt</sup>Filip 5, 31-150 Krakow, Poland,*  
Institute of Physics, Pedagogical University, 30-084 Krakow, Poland\*

Z. Ropka

Center of Solid State Physics, *S<sup>nt</sup>Filip 5, 31-150 Krakow, Poland*

Magnetic properties of stoichiometric  $\text{YTiO}_3$  has been calculated within the single-ion-based paradigm taking into account the low-symmetry crystal field and the intra-atomic spin-orbit coupling of the  $\text{Ti}^{3+}$  ion. Despite of the very simplified approach the calculations reproduce perfectly the value of the magnetic moment and its direction as well as temperature dependence of the magnetic susceptibility  $\chi(T)$ . It turns out that the spin-orbit coupling is fundamentally important for 3d magnetism and magnetic properties are determined by lattice distortions.

PACS numbers: 75.25.+z, 75.10.Dg

Keywords: Crystalline Electric Field, 3d oxides, magnetism, spin-orbit coupling,  $\text{YTiO}_3$

## INTRODUCTION

$\text{YTiO}_3$  is a unique 3d ferromagnet [1, 2, 3] - the most of oxides are antiferromagnetic. In combination with a rather simple perovskite structure and  $\text{Ti}^{3+}$  ions expected to have one electron in the incomplete 3d shell,  $\text{YTiO}_3$  is regarded to be very good exemplary system for studying basic interactions in 3d oxides. Despite this simplicity its properties are not understood yet. In fact, there is going on at present a hot debate on description of its magnetic and electronic properties [4, 5, 6, 7, 8, 9, 10, 11, 12, 13, 14, 15, 16, 17, 18, 19, 20]. A time when such system was treated as a  $S=1/2$  system i.e. with the spin-only magnetism and the fully quenched orbital magnetism is already gone. Also the simplest versions of the band picture turned out to be completely useless giving already at the start disagreement with experiment predicting a metallic ground state whereas  $\text{YTiO}_3$  is in the reality a good insulator.

$\text{YTiO}_3$ , when stoichiometric, is very good insulator. Its resistivity at room temperature amounts to  $5 \cdot 10^{-2}$   $\Omega\text{cm}$  [11]. The resistivity rapidly grows up with decreasing temperature. It is ferromagnetic below  $T_c$  of 30-35 K [3, 4]. The macroscopic magnetisation, if recalculated per the formula unit, points to a moment of  $0.84 \mu_B$  [3]. The paramagnetic susceptibility has been found to follow the Curie-Weiss law with  $\theta = 39$  K, if subtracted a diamagnetic and temperature independent orbital contributions of a total size of  $0.351 \cdot 10^{-3}$  emu/mol.

The aim of this paper is to present results of single-ion based calculations of properties of  $\text{YTiO}_3$ . Our single-ion results seem to be quite remarkable. We took into account low-symmetry off-octahedral crystal-field (CEF) interactions and the intra-atomic spin-orbit (s-o) coupling, that turn out to be of the comparable strength.

## THEORETICAL OUTLINE

We consider exactly stoichiometric  $\text{YTiO}_3$ . From this and the insulating ground state we infer that all Ti ions are in the trivalent state according to the charge distribu-

tion  $\text{Y}^{3+}\text{Ti}^{3+}\text{O}_3^{2-}$ . The relevant charge transfer occurs during the formation of the compound. In the perovskite-based structure of  $\text{YTiO}_3$  the  $\text{Ti}^{3+}$  ion is surrounded by six oxygen ions forming distorted octahedron. There are still some Ti ions at the surface, for instance, with a reduced symmetry, but they are generally neglected, because we are interested in intrinsic properties of  $\text{YTiO}_3$ . The local octahedra in  $\text{YTiO}_3$  are tilted and rotated, what causes the need for consideration a larger elementary cell, with four Ti ions instead of one as in the simple perovskite structure. Thanks it other three Ti ions get a crystallographic freedom. As a result of rotations, tilts and other atom displacements there are four short Ti-O bonds and two long Ti-O bonds.

The orthorhombic lattice in the  $Pbnm$  structure results from that of an ideal cubic perovskite by setting  $a_o = \sqrt{2} a_c$ ,  $b_o = \sqrt{2} a_c$  and  $c_o = 2a_c$ , where  $a_c$  denotes the lattice parameter of the simple cubic perovskite.  $a_c$  is of order of 400 pm.

In the  $Pnma$  structure used by some authors the doubling occurs along the  $b$  direction. The  $c$ ,  $a$ , and  $b$  axis in the  $Pnma$  structure becomes the  $a$ ,  $b$  and  $c$  axis in the  $Pbnm$  structure, respectively. Independently of the used  $Pbnm$  or  $Pnma$  space group the derivation of the local surroundings must be, of course, the same.

Here we use the  $Pbnm$  space group. Then the easy magnetic axis is the  $c$  axis, [3]. The lattice parameters at  $T = 293$  K, according to Ref. 2, cited by [5, 15], are:  $a_o = 531.6$  pm,  $b_o = 567.9$  pm and  $c_o = 761.1$  pm. These parameters have been confirmed by detailed structural measurements of Loa *et al.* [19].

Cwik *et al.* [5] have derived the respective bonds: 207.7 pm (Ti-O(b)), 201.6 pm (Ti-O(a)) and the apical bond 202.3 pm (Ti-O(c)). Loa *et al.* [19] have measured influence of the external pressure on these bonds. From these crystallographic studies we get an input to our theoretical considerations that the lattice surroundings of the Ti ion in  $\text{YTiO}_3$  is predominantly octahedral with a slight

orthorhombic distortion.

## RESULTS AND DISCUSSION

The electronic structure of the  $Ti^{3+}$  ion with one  $d$ -electron under the action of the crystal-field interactions  $H_{CF}$  and in the presence of the intra-atomic spin-orbit coupling  $H_{s-o}$  we calculated with the use of the single-ion-like Hamiltonian often used in description of  $3d$  impurity states in the Electron Paramagnetic Resonance [22, 23, 24], which we accept also for a solid, where  $3d$  atom is the full part of the crystallographic structure:

$$H_d = H_{CF} + H_{s-o} = B_4(O_4^0 + 5O_4^4) + \lambda_{s-o}L \cdot S + B_2^0O_2^0 + \mu_B(L + g_e S) \cdot B_{ext}. \quad (1)$$

The calculated electronic structure is presented in Fig. 1. The crystal field has been divided into the cubic part, usually dominant in case of compounds containing  $3d$  ions, and the off-octahedral distortion written by the second-order leading term  $B_2^0O_2^0$ . The last term, Zeeman term, allows calculations of the influence of the external magnetic field.  $g_e$  amounts to 2.0023. The Zeeman term is necessary for calculations, for instance, of the paramagnetic susceptibility - in fact the paramagnetic susceptibility is customarily calculated [25] as the magnetization in an external field of, say, 0.1 T applied along different crystallographic directions.

The detailed form of the Hamiltonian (1) is written down in the LS space that is the 10 dimensional spin-orbital space  $|LSL_zS_z\rangle$ . The  $L$  and  $S$  quantum numbers for one  $3d$  electron are equal to  $L=2$  and  $S=1/2$  (here, for  $3d^1$  configuration, lower  $l$  and  $s$  could be also used). The Hamiltonian (1) is customarily treated by perturbation methods owing to the weakness of the  $s$ - $o$  coupling for the  $3d$  ions in comparison to the strength of the crystal-field interactions. We have accepted the weakness of the  $s$ - $o$  coupling, what is reflected by the sequence of terms in the Hamiltonian (1), but we have performed direct calculations treating all shown terms in the Hamiltonian (1) on the same footing. The separate figures, if presented, are shown for the illustration reasons.

Diagonalization have been performed for physically relevant values of  $\lambda_{s-o}$  of  $+220$  K ( $= 150 \text{ cm}^{-1}$ ) found for the  $Ti^{3+}$  ion [21]. The cubic CEF parameter  $B_4$  is taken as  $+240$  K (results are not sensitive to its exact value provided  $B_4 > +50$  K). The positive sign of  $B_4$  comes from *ab initio* point charge calculations of octupolar interactions of the  $Ti^{3+}$  ion with the octahedral oxygen (negative charges) surroundings. Such value of  $B_4$  yields the  $T_{2g}$ - $E_g$  splitting of 2.5 eV. A splitting of 2.15-2.5 eV has been observed for  $Ti^{3+}$  ions in  $Al_2O_3$ , where the similar oxygen octahedron exists. In  $LaCoO_3$  we derived value of  $B_4$  of 280-320 K [26].

In Fig. 2 we show detailed calculations of the influence of the spin-orbit coupling on the three lowest states  $t_{2g}$  ( $=^2T_{2g}$ ) of the  $3d^1$  configuration for the elongated

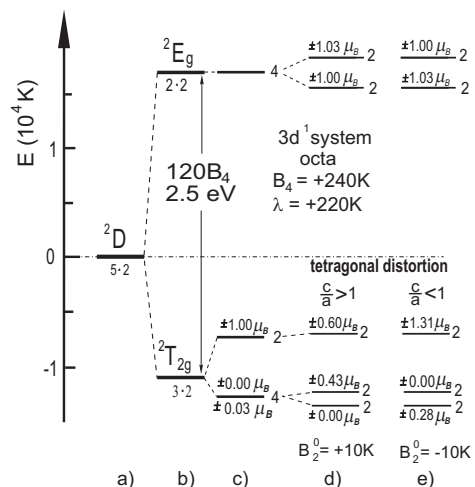


FIG. 1: The calculated fine electronic structure of the  $3d^1$  electronic system ( $Ti^{3+}$ ,  $V^{4+}$  ions) in the paramagnetic state under the action of the crystal field and spin-orbit interactions: a) the 10-fold degenerated  $^2D$  term realized in the absence of the CEF and the  $s$ - $o$  interactions; b) the splitting of the  $^2D$  term by the octahedral CEF surrounding  $B_4=+240$  K ( $\lambda_{s-o}=0$ ) yielding the  $^2T_{2g}$  cubic subterm as the ground state; c) the splitting of the lowest  $^2T_{2g}$  cubic subterm by the combined octahedral CEF and spin-orbit interactions ( $B_4=+240$  K and  $\lambda_{s-o}=+220$  K); the degeneracy and the associated magnetic moments are shown; d) the splitting due to the elongated tetragonal off-octahedral distortion of  $B_2^0=+10$  K ( $c/a>1$ ); e) the splitting due to the compressing tetragonal distortion of  $B_2^0=-10$  K ( $c/a<1$ , apical oxygens become closer). Figs c, d and e are not to the left hand energy scale - the splitting of the three lowest states on Figs c, d and e amounts to 333 K, 368 K and 372 K, respectively.

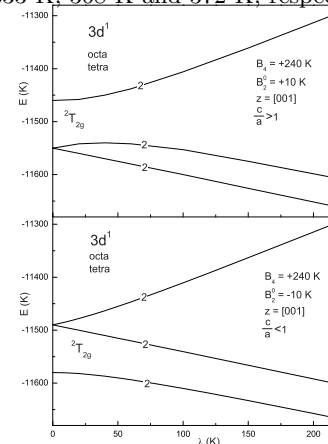


FIG. 2: The calculated spin-orbit coupling  $\lambda$  dependence of the three lowest states  $t_{2g}$  ( $=^2T_{2g}$ ) of the  $3d^1$  configuration for the elongated ( $c/a>1$ ) and stretched ( $c/a<1$ ) tetragonal off-octahedral distortion. The right hand states correspond to the three lowest states shown in Fig. 1d and 1e.

( $c/a>1$ ) and stretched ( $c/a<1$ ) tetragonal off-octahedral distortion, realized for  $B_2^0 > 0$  and  $B_2^0 < 0$ , respectively. Analyzing the effect of the sign of the tetragonal distortion lead us to a conclusion that the magnetic moment lies along the tetragonal axis for the  $z$ -axis stretching. For the elongation case the moment lies perpendicularly

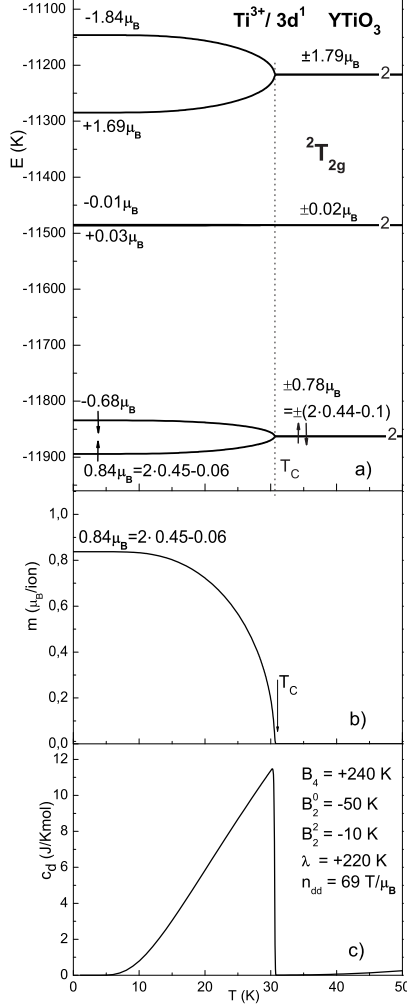


FIG. 3: The calculated temperature dependence of some properties of YTiO<sub>3</sub>. a) the temperature dependence of the three lowest states ( $t_{2g}$  states) of the Ti<sup>3+</sup>-ion in YTiO<sub>3</sub> in the magnetically-ordered state below  $T_c$  of 30.6 K; in the paramagnetic state the electronic structure is temperature independent unless we do consider a changing of the CEF parameters, for instance, due to the thermal lattice expansion. The used parameters:  $B_4 = +240$  K,  $B_2^0 = -50$  K,  $B_2^2 = -10$  K,  $\lambda_{s-o} = +220$  K and  $n_{d-d} = 69$  T/ $\mu_B$ . The splitting of the Kramers doublets should be noticed in the ferromagnetic state. Excited states are at 377, 645, 28843 and 29447 K. (b) the temperature dependence of the Ti<sup>3+</sup>-ion magnetic moment in YTiO<sub>3</sub>. At 0 K the total moment  $m_{Ti}$  of  $0.84 \mu_B$  is built up from the orbital  $m_o$  and spin  $m_s$  moment of  $-0.06$  and  $0.90 \mu_B$ , respectively. (c) The calculated temperature dependence of the  $3d$  contribution  $c_d(T)$  to the heat capacity of YTiO<sub>3</sub>. The  $\lambda$ -type peak marks  $T_c$ .

to the tetragonal axis. Taking into account that in YTiO<sub>3</sub> the ordered moment lies along the  $c$  direction (in the  $Pbnm$  structure) and our long-lasting studies of CEF effects [16, 17, 27, 28] we came to values for  $B_2^0 = -50$  K and  $B_2^2 = -10$  K which reproduce the magnetic moment value, its direction and (some) thermodynamics. The

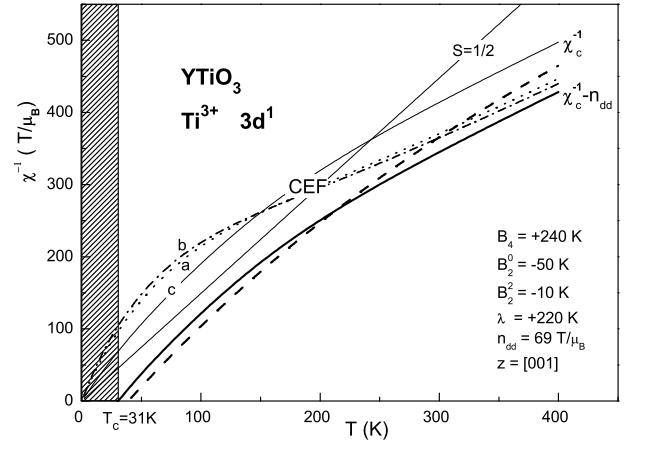


FIG. 4: Calculated temperature dependence of the paramagnetic susceptibility  $\chi(T)$  for the  $3d^1$  system Ti<sup>3+</sup> in YTiO<sub>3</sub> for three different crystallographic directions ( $a$ ,  $b$ , and  $c$ ) calculated for  $B_4 = +240$  K,  $B_2^0 = -50$  K,  $B_2^2 = -10$  K and  $\lambda_{s-o} = +220$  K; these curves are denoted with CEF. The lowest solid line is the  $\chi_c(T)$  dependence calculated with taking into account the ferromagnetic interactions with  $n_{d-d} = 69$  T/ $\mu_B$  - this curve should be compared with experimental data, taking after Ref. [4], are shown by the lowest dashed line. The shadow area indicates the ferromagnetic state. The straight line denoted with  $S = 1/2$  shows the Curie law expected for the free  $S = 1/2$  spin.

calculated ground-state eigenfunction (the  $z$  component of  $L$  and  $S$  are shown)

$$\psi_{GS\pm} = 0.690|\pm 2, \mp \frac{1}{2}\rangle - 0.678|\mp 2, \mp \frac{1}{2}\rangle - 0.253|\pm 1, \pm \frac{1}{2}\rangle - 0.020|\mp 1, \pm \frac{1}{2}\rangle \quad (2)$$

where the sign  $\pm$  refers to two conjugate Kramers states. This state has  $S_z = \mp 0.44$  and  $L_z = \pm 0.10$ . The resultant moment  $m_z = \pm 0.78 \mu_B$  cancels each other in the paramagnetic state as is denoted in Fig. 3a.

Making use of the  $|xy, \mp\rangle$  function extended for the spin component, as  $|xy, \mp\rangle = \sqrt{1/2}(|2, \mp \frac{1}{2}\rangle - |-2, \mp \frac{1}{2}\rangle)$  (also functions  $|xz\rangle$ ,  $|yz\rangle$ ,  $|x^2 - y^2\rangle$  and  $|z^2\rangle$ ) one can write the ground state  $\psi_{GS\pm}$  function approximately as:

$$\psi_{GS\pm} = 0.967|xy, \mp\rangle + 0.0085|x^2 - y^2, \mp\rangle - 0.186|xz, \pm\rangle - 0.172|yz, \pm\rangle + \dots \quad (3)$$

In the magnetic state the ground state  $\psi_{GS\pm}$  Kramers doublet function becomes polarized as a molecular field is self-consistently settled down and the function

$$\psi_{GS+} = 0.695|+2, -\frac{1}{2}\rangle - 0.686|-2, -\frac{1}{2}\rangle - 0.215|+1, +\frac{1}{2}\rangle - 0.016|-1, +\frac{1}{2}\rangle \quad (4)$$

is obtained as the ground state. The higher conjugate state is calculated to be described by

$$\psi_{GS-} = 0.665|+2, +\frac{1}{2}\rangle - 0.682|-2, +\frac{1}{2}\rangle + 0.303|-1, -\frac{1}{2}\rangle + 0.026|+1, -\frac{1}{2}\rangle \quad (5).$$

Below  $T_c$  there opens, as is seen in Fig. 3a, a spin-like gap that amounts at  $T = 0$  K to  $59.7$  K ( $= 41.4$   $\text{cm}^{-1} = 5.15$  meV). The spin-like gap is associated with the splitting of the Kramers doublet ground state in the ferromagnetic state. The magnetic ground state  $\psi_{GS+}$  has  $S_z = -0.45$  and  $L_z = +0.06$  and the resultant moment amounts to  $0.84 \mu_B$ . The appearance of the magnetic state is calculated self-consistently. It appears in the instability temperature ( $T_c$ ) in the temperature dependence of the CEF paramagnetic susceptibility when

$$\chi_{CF}^{-1}(T_c) = n_{d-d} \quad (6)$$

as is illustrated in Fig. 4 for different crystallographic directions. With decreasing temperature this equality is reached the first for the  $c$  direction pointing the preferred magnetic arrangement axis. The magnetic state is calculated self-consistently by adding to the Hamiltonian Eq. (1) the inter-site magnetic (spin-dependent) interactions instead of the last Zeeman term [29]

$$H_{d-d} = n_{d-d} \left( -m_d \cdot m_d + \frac{1}{2} \langle m_d^2 \rangle \right) \quad (7)$$

where  $n_{d-d}$  is the molecular-field coefficient.

Having eigenvalues in a function of temperature we calculate the free energy  $F(T)$ . From  $F(T)$  using well-known statistical formulae we calculate all thermodynamics like temperature dependence of the magnetic moment, of the additional  $c_d$  heat capacity, of paramagnetic susceptibility, of the  $3d$ -shell quadrupolar moment and many others. The present calculations are similar to those performed for  $\text{FeBr}_2$  [30] and  $\text{CoO}$  [31].

### CONCLUSIONS

We have calculated consistently a value of the magnetic moment of  $0.84 \mu_B$  and its direction (along the  $c$  axis in the Pbnm structure) in  $\text{YTiO}_3$  as well as temperature dependence of the paramagnetic susceptibility in very good agreement with experimental observations.

This remarkable reproduction of so many physical properties has been obtained within the localized-electron approach taking into account lattice off-octahedral distortions and the intra-atomic spin-orbit coupling [25]. Although the spin-orbit coupling is weak, it amounts to only 1.2 % of the octahedral CEF splitting, it has enormous influence on the low-energy electronic structure and low-temperature magnetic and electronic properties. The spin-orbit coupling binds the orbital moment to the spin moment being the reason for the spin-lattice and spin-phonon coupling. The suggested energy positions of the excited CEF states have to be verified by experiment. The good reproduction of the paramagnetic susceptibility indicates on the proper overall splitting of the  $t_{2g}$  states - one should note that our splitting is about 5 times smaller than that obtained in Refs [8, 9, 12, 14]. We are aware that our calculations have to be extended to take into account many other effects - first of them seems to be geometrical effects associated with the non-collinearity of the local symmetry axes, but these studies

prove that magnetic properties of  $\text{YTiO}_3$  are predominantly determined by the atomic-scale lattice distortions, crystal-field and the spin-orbit coupling of the  $\text{Ti}^{3+}$  ions, whereas charge fluctuations are negligible. An interplay of the spin-orbit coupling, lattice distortions and magnetic order is very subtle involving rather small energies, smaller than 5 meV making theoretical studies quite difficult.

We point out that all discussed by us parameters are physical measurable parameters. The  $B_2^0$  and  $B_2^2$  parameters are related to the observed orthorhombic local surroundings. A negative value of the  $B_2^0$  parameter results from the stretching of the apical bonds with respect to the average bond length within the  $a-b$  plane. The  $B_2^2$  parameter is related to the difference in the  $a-b$  plane. A success of our ionic approach, called due to extension to the magnetic state a quantum atomistic solid-state theory (QUASST) [32], if applied to  $\text{YTiO}_3$ , is related to our long-lasting systematic studies, despite of discrimination and inquisition, of the spin-orbit coupling and crystal-field interactions in  $3d$  compounds and in study of the region, where the spin-orbit coupling and off-octahedral lattice distortions are of the comparable strength.

**Acknowledgements.** We are very grateful to all our opponents. Although we do not think that the discrimination and inquisition should take place in Physics at the XXI century their critics largely stimulated these, very natural for us studies. This discrimination is the best proof that the knowledge about the CEF and the role of the spin-orbit coupling in  $3d$  magnetism is rather poor. We are thankful to a numerous members of the International Committee of the Strongly-Correlated Electron Systems Conference in Vienna 2005 for the friendly support. We are convinced that Physics can develop only in the friendly atmosphere and in the open exchange of information.

♣ dedicated to John Van Vleck and Hans Bethe, pioneers of the crystal-field theory, to the 75<sup>th</sup> anniversary of the crystal-field theory, and to Pope John Paul II, a man of freedom and honesty in life and in Science.

---

\* URL: <http://www.css-physics.edu.pl>; Electronic address: sradwan@cyf-kr.edu.pl

- [1] J. E. Greedan, *J. Less-Common Met.* **111**, 335 (1985).
- [2] D. A. MacLean, H. N. Ng, and J. E. Greedan, *J. Solid State Chem.* **30**, 35 (1979); D. A. MacLean, K. Seto, and J. E. Greedan, *J. Solid State Chem.* **40**, 241 (1981).
- [3] M. Tsubota, F. Iga, T. Takabatake, N. Kikugawa, T. Suzuki, I. Oguro, H. Kawanaka, and H. Bando, *Physica* **281/282**, 622 (2000).
- [4] M. Itoh, M. Tsuchiya, H. Tanaka, and K. Motoka, *J. Phys. Soc. Jap.* **68**, 2783 (1999).
- [5] M. Cwik, T. Lorenz, J. Baier, R. Muller, G. Andre, F. Bouree, F. Lichtenberg, A. Freimuth, R. Schmitz, E. Muller-Hartmann, and M. Braden, *Phys. Rev. B* **68**,

- 060401(R) (2003); cond-mat/0302087.
- [6] E. Pavarini, S. Biermann, A. Poteryaev, A. I. Lichtenstein, A. Georges, and O. K. Andersen, Phys. Rev. Lett. **92**, 176403 (2004); cond-mat/0309102.
- [7] G. Khaliullin and S. Okamoto, Phys. Rev. B **68**, 205109 (2003); cond-mat/0510175.
- [8] R. M. Eremina, M. V. Eremin, S.V. Iglamov, J. Hemberger, H.-A. Krug von Nidda, F. Lichtenberg, and A. Loidl, cond-mat/0407264.
- [9] S. V. Streltsov, A. S. Mylnikova, A. O. Shorikov, Z. V. Pchelkina, D. I. Khomskii, and V. I. Anisimov, Phys. Rev. B **71**, 245114 (2005); cond-mat/0504281.
- [10] R. Ruckamp, E. Benckiser, M. W. Haverkort, H. Roth, T. Lorenz, A. Freimuth, L. Jongen, A. Moller, G. Meyer, P. Reutler, B. Buchner, A. Revcolevschi, S-W Cheong, C. Sekar, G. Krabbes, and M. Gruninger, N. J. Phys. **7**, 144 (2005); cond-mat/0503405.
- [11] Y. Taguchi, Y. Tokura, T. Arima, and F. Inaba, Phys. Rev. B **48**, 511 (1993).
- [12] M. W. Haverkort, Z. Hu, A. Tanaka, G. Ghiringhelli, H. Roth, M. Cwik, T. Lorenz, C. Schussler-Langeheine, S. V. Streltsov, A. S. Mylnikova, V. I. Anisimov, C de Nadai, N. B. Brookes, H. H. Hsieh, H. -J. Lin, C. T. Chen, T. Mizokawa, Y. Taguchi, Y. Tokura, D. I. Khomskii, and L. H. Tjeng, Phys. Rev. Lett. **94**, 056401 (2005).
- [13] R. Schmitz, O. Entin-Wohlman, A. Aharony, E. Muller-Hartmann, cond-mat/0506328.
- [14] I. V. Solov'yev, Phys. Rev. B **69**, 134403 (2004).
- [15] H. Fujitani and S. Asano, Phys. Rev. B **51**, 2098 (1995).
- [16] Z. Ropka, R. Michalski, and R. J. Radwanski, cond-mat/9907141.
- [17] R. J. Radwanski, R. Michalski, and Z. Ropka, Physica B **312-313**, 628 (2002).
- [18] C. Ulrich, G. Khaliullin, S. Okamoto, M. Reehuis, A. Ivanov, H. He, Y. Taguchi, Y. Tokura, and B. Keimer, Phys. Rev. Lett. **89**, 167202 (2002).
- [19] I. Loa, X. Wang, K. Syassen, H. Roth, T. Lorenz, M. Hanfland, and Y. -L. Mathis, cond-mat/0504383.
- [20] M. Imada, A. Fujimori, and Y. Tokura, Rev. Mod. Phys. **70**, 1039 (1998).
- [21] NIST Atomic Spectra Database, in <http://physics.nist.gov> gives an energy of the  $^2D_{5/2}$  multiplet of  $382.1 \text{ cm}^{-1}$  above the ground multiplet  $^2D_{3/2}$ . It yields  $\lambda_{so}$  of  $152.8 \text{ cm}^{-1} = 19.0 \text{ meV}$  or  $220.0 \text{ K}$ .
- [22] A. Abragam and B. Bleaney, *Electron Paramagnetic Resonance of Transition Ions* (Clarendon Press, Oxford) (1970), ch. 7.
- [23] C. Ballhausen, in: *Ligand Field theory* (McGraw-Hill) (1962).
- [24] W. Low, in: *Paramagnetic Resonance in Solids* (Academic Press) (1960).
- [25] the computer program is available on the written request to the authors.
- [26] Z. Ropka and R. J. Radwanski, Phys. Rev. B **67**, 172401 (2003).
- [27] R. J. Radwanski and Z. Ropka, cond-mat/9907140.
- [28] R. J. Radwanski, J. Phys.: Condens. Matter **8**, 10467 (1996).
- [29] the use of the spin-spin Hamiltonian lead to similar results - we checked it getting  $n_{ex} = 63.75 \text{ T}/\mu_B$  in accordance with the scaling of  $n_{d-d}$  with the spin/total moment ratio.
- [30] Z. Ropka, R. Michalski, and R. J. Radwanski, Phys. Rev. B **63**, 172404 (2001).
- [31] R. J. Radwanski and Z. Ropka, Physica B **345**, 107 (2004), cond-mat/0306695.
- [32] R. J. Radwanski, R. Michalski, and Z. Ropka, Acta Phys. Pol. B **31**, 3079 (2000); cond-mat/0010081.